Rheol Acta (2005) 44: 352–359
DOI 10.1007/s00397-004-0416-1

ORIGINAL CONTRIBUTION

Dawn R. Arda
Malcolm R. Mackley

Sharkskin instabilities and the effect of slip from gas-assisted extrusion

Received: 1 March 2004
Accepted: 12 August 2004
Published online: 12 January 2005

D. R. Arda · M. R. Mackley (✉)
Department of Chemical Engineering,
University of Cambridge, Pembroke Street,
Cambridge, CB2 3RA, UK
E-mail:
malcolm_mackley@cheng.cam.ac.uk
Tel.: +44-1223-334777
Fax: +44-1223-334796

Abstract This paper is concerned with a polymer extrusion instability and the effect of introducing slip by means of a thin lubricating gas layer between the extrusion die wall and the flowing polymer melt. Gas-assisted extrusion (GAE) experiments were carried out using high-density polyethylene (HDPE) and linear low-density polyethylene (LLDPE) for a number of different gas injection die geometries. The stress distributions within the polymer melt were monitored during extrusion using flow birefringence. Polyflow numerical simulations were used to calculate the local stress concentrations in the melt at the die exit, as these were believed to be related to the occurrence of sharkskin. Simulations were also used to observe the effect of a full slip boundary condition as imparted by GAE. A key finding of the paper is that GAE in the parallel section of the die wall simply moved the local exit stress concentration upstream to the point of gas injection, and therefore did not reduce sharkskin. Simulations indicated that for correctly designed dies, the local surface stress concentration would be reduced. However, it was found experimentally that it was not possible to obtain a stable gas layer for this die design with upstream gas injection. A numerical investigation, involving simulations of varying levels of partial slip along the die wall, indicated an optimum level of slip where the stress concentrations were reduced. It is speculated that this is the reason that coatings such as PTFE, which impart a partial slip, can reduce sharkskin while GAE does not. The findings show that a controlled level of partial slip lowers the overall stress concentrations.

Keywords Sharkskin · Instability · Gas-assisted extrusion · Slip · Polyethylene

Introduction

Sharkskin instabilities are small-amplitude, high frequency surface defects that occur on the surface of certain polymers at high processing rates. The instability can limit the production rates of polymers such as linear low-density polyethylene (LLDPE) and high-density polyethylene (HDPE), for processes such as extrusion. The subject has been extensively reviewed by Tordella [1], Petrie and Denn [2], Larson [3], Wang [4] and Denn [5–7]. Although there is controversy over the precise mechanism behind the instability, it is generally agreed that sharkskin originates at the die exit. A growing number of researchers believe that the instability is related to local stress concentrations that occur in the melt in the region where the polymer emerges from the die (see for example [8]). The stress concentration arises due to the abrupt change in boundary conditions at the die exit. The abrupt change is due to the polymer melt at the die wall near the exit being forced to accelerate

from a near zero velocity to the velocity of the bulk polymer downstream of the exit. This gives rise to a sharp stress concentration within the melt in this area.

Studies involving die wall coatings that promote slip (for example PTFE, [9]) and slip additives [10], have shown that it is possible to delay or even eliminate sharkskin by providing slip along the die wall. Research has therefore been undertaken to establish the effect of slip from gas-assisted extrusion (GAE) on sharkskin. GAE involves the injection of gas to form a uniform boundary layer between an extrusion die wall and a flowing polymer melt. As the polymer melt is extruded through the die, gas is injected through a small slot in the side of the die. Previous studies by Liang and Mackley [11] showed that the gas gives rise to an essentially full slip boundary condition and modifies the stress field at the boundary and exit of the die. It was also found to significantly reduce the magnitude of die swell [11]. The gas forms a layer between the melt and the die wall that "lubricates" the flow of the melt and completely removes polymer contact with the wall. The gas layer effectively removes all the shear stress at the side of the melt, thereby eliminating the local stress concentration at the die exit. This paper explores whether GAE is able to eliminate sharkskin and examines the results of numerical simulations used to determine the effect of different levels of wall slip.

Experimental

Materials

The materials studied were Rigidex HD5502XA HDPE supplied by BP Chemicals and Dowlex NG5056E LLDPE supplied by Dow Benelux B.V. Material properties of both polymers are given in Table 1 and their rheological parameters at the extruded temperatures are given in Table 2. Rigidex is a commercial polymer used for blow-moulded containers and packaging. Dowlex LLDPE is a heterogeneous blend of linear polyethylene and polyethylene chains with varying numbers of octene-1 branches. Its main application is in blown film extrusion. Further details on how the material properties were obtained can be found in Arda [12].

Table 1 Material properties of Rigidex HDPE and Dowlex LLDPE

	Material	
	Rigidex HD5502XA	Dowlex NG5056E
Supplier	BP Chemicals	Dow Benelux B.V.
Polymer	HDPE	LLDPE
Density (g/cm^3)	0.954	0.9195
Mn (g/mol)	20,600	54,800
Mw (g/mol)	141,600	113,000
Mw/Mn	6.87	2.1

Table 2 Spectrum coefficients g_i, λ_i and damping factors k for Rigidex HDPE and Dowlex LLDPE

Rigidex HDPE		Dowlex LLDPE	
λ_i (s)	g_i (Pa)	λ_i (s)	g_i (Pa)
0.002	125,000	0.0021	243,000
0.0094	92,000	0.0095	144,000
0.044	37,500	0.043	53,400
0.21	21,000	0.20	12,500
0.97	8,040	0.89	2,080
4.54	4,130	4.04	283
21.3	771	18.4	22.4
100	1,200	83.3	0.0000096
$k = 0.25 \pm 0.02$		$k = 0.21 \pm 0.02$	

Extrusion

The experimental apparatus used to carry out extrusion experiments consisted of a 25-mm single screw extruder that was equipped with a melt gear pump, which was designed to control the flow rate and the extruder screw speed through a pressure feedback system. The dies were held in a stainless steel flowcell that accommodated optical windows for flow birefringence purposes. The flowcell allowed interchangeable die inserts. The polymer extrudate was hauled off vertically using a haul-off machine with controllable rotational speed.

Two types of gas injection slit dies were investigated. Die I, shown in Fig. 1, was a 90° contraction parallel

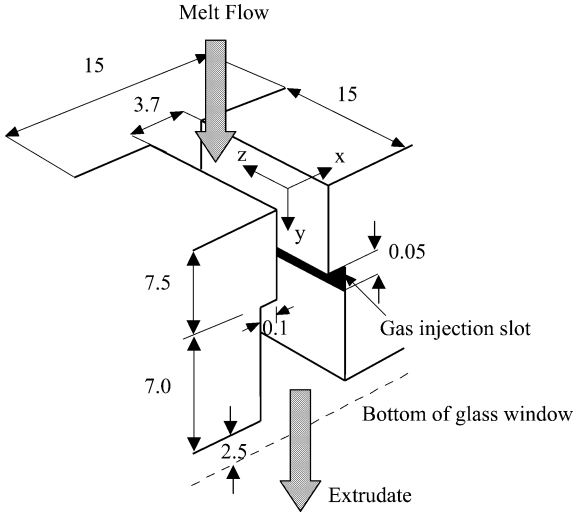

Fig. 1 Die I: die depth 15 mm, slit length 14.5 mm, downstream gap width 3.9 mm. *Dotted lines* indicate the edges of the optical windows. x is the width direction, y is the flow direction and z is the depth direction. All dimensions are in millimetres

slit die with a die length of 14.5 mm and a downstream extrusion gap width of 3.9 mm. Gas injection was via a 50-μm slot across the die walls, 7 mm from the die exit. The gas reached the 50-μm slot through a cavity area at the back of each die. This allowed some heating of the gas before it entered the die. It was possible that there was not enough time for the gas to be heated to the same temperature as that of the melt, and thus the gas may have had a slight cooling effect on the melt and die wall. Downstream of the gas slots, an instep of 0.1 mm was found to be necessary to facilitate the formation of a stable gas layer. Further details of this die and the extruder rig can be found in Liang and Mackley [11]. The second type of die, Die II, shown in Fig. 2, had a radiused entry and the gas injection slots were positioned upstream of the die contraction. Die inserts were polished using a fine brass wire brush prior to use.

The GAE apparatus used nitrogen gas in two symmetrical streams supplied at room temperature from a storage cylinder. Each gas stream passed through a pressure reduction valve that reduced the pressure from 200 to 40 bar and then through a needle valve to control the flow rate such that the gas injection pressure was in the region of 0–10 bar gauge. Extrudate samples were analysed using a Leica Stereoscan 430 scanning electron microscope.

Flow rates in this paper are given in RPM, corresponding to the melt gear pump speed. The corresponding mass flow rates can be found using the plot in Fig. 3.

Flow birefringence

The flow cell was designed to accommodate optical windows that enabled flow birefringence measurements to be made (see Fig. 4). Monochromatic light was provided by a mercury lamp and a 546-nm wavelength (green) filter. The flow cell was placed between a polariser, oriented at 45° with respect to the principle flow direction, and an analyser, oriented at −45°. The transmitted picture of dark and light bands was captured by a CCD camera and recorded onto video.

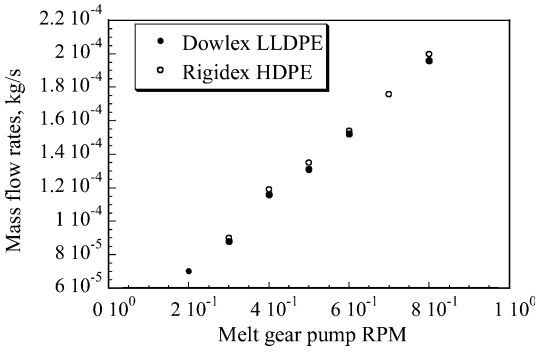

Fig. 3 Plot of mass flow rate versus melt gear pump speed for Rigidex HDPE at 180 °C and Dowlex LLDPE at 190 °C through Die I. Mass flow rates do not vary significantly between Die I and Die II

Numerical simulation

Numerical simulations were carried out using Polyflow, a commercial finite element CFD package developed by Crochet and Walters [13]. The package was used in combination with a multimode K-BKZ integral equation with the Wagner irreversible damping factor. Polyflow numerical simulations were used to predict principal stress difference (PSD) values in the melt flowing through the die. The simulations were carried out for a polymer flow rate of 2.4×10^{-7} m^3/s, which was experimentally observed to be within a sharkskin regime. Rheological data used in the simulation are given in Table 2 and consisted of an eight-mode linear viscoelastic spectrum together with a single irreversible damping factor, k. The 0.1-mm instep downstream of the gas injection point was neglected to avoid the numerical convergence difficulties that were encountered with the instep present. A 1,732 element mesh was used for Die I with local refinement at the

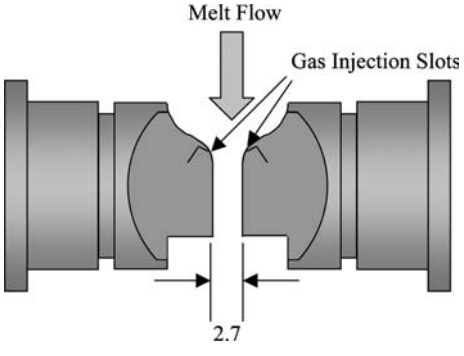

Fig. 2 Die II: die depth 15 mm, extrusion gap width 2.7 mm. Dimensions are in millimetres

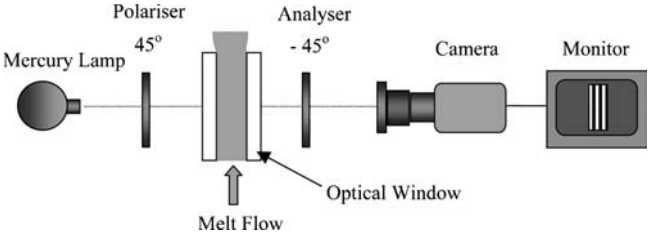

Fig. 4 Optics set-up for flow birefringence

corners and refinement to element sizes of 30×30 μm at the die exit.

The finite element formulation in Polyflow used quadratic interpolation for velocities and linear interpolation for pressure. The boundary conditions assumed were a fully-developed flow 25 mm upstream of the slit entrance, no slip at the die wall without gas, full slip at the wall with gas, symmetry along the centre plane, and an 80-mm long free surface at the outlet. The convergence criterion was set to 10^{-3} .

At the downstream exit without gas injection, the separation point is a node where the metal edge, molten polymer and air meet. This was modelled as a zero slip boundary at the edge and a free boundary between polymer and air, downstream of the edge. In the case of gas injection, the separation node is where the metal edge, molten polymer and injection gas meet. Experimentally, downstream of this node there is a constrained boundary between the injection gas and the polymer. In the case of the simulation, this was modelled as a flat surface with a full slip boundary condition.

A mesh sensitivity study investigated three meshes with 1,732, 2,056 and 2,382 elements respectively. The meshes were refined such that the elements immediately at the wall at the exit were 30×30, 20×20 and 15×15 μm respectively. Mesh sensitivity was investigated by qualitatively comparing the streamlines and global stress contours and quantitatively comparing the pressure difference, velocities and stresses along the centreline and the PSD along streamlines close to the die wall. These were found to match across the three dies. The exit PSD peaks along streamlines 50 μm from the die wall were found to agree to within 2%. This was considered adequate and subsequent simulations were carried out with meshes having exit element sizes of 30×30 μm.

A difference in solutions between the three meshes only occurred in the element closest to the wall at the exit. This was a consequence of a stress singularity at the die exit (see for example [14, 15]). It was found that the more refined the mesh, the higher the numerically-predicted stress in the one node adjacent to the wall. It may, however, be concluded that mesh independence was obtained in the simulations outside the element immediately adjacent to the wall, which in this case was 30 μm for the coarsest mesh.

Numerical simulations were used to investigate the effect of partial slip on the stress concentrations. The simplest law available in Polyflow was used, defined as:

$$f_s = -f_{slip} \cdot v_s \quad (1)$$

where f_s is the friction at the wall, v_s is is the velocity tangential to the wall and f_{slip} is a slip coefficient. A value of $f_{slip} = 0$ is equivalent to full slip, and the higher the value the lower the level of slip. Simulations were carried out with values of f_{slip} varying from 0 to 1×10^8.

Results and discussion

Gas-assisted extrusion

Die I

Experiments using Die I were carried out using both Rigidex HDPE and Dowlex LLDPE. The initial breakthrough gas pressure that was required was in the region of 20 bar, while the subsequent stable gas pressures required were much lower. Stable and uniform gas layers were observed through the optical windows at the sides of the die. Flow birefringence results using this die at a moderately high flow rate, both without and with gas, for Rigidex HDPE are shown in Fig. 5.

Figure 5a shows that, under normal extrusion conditions without gas, the fringes and therefore the stresses in the die are parallel to the die wall. This corresponds to an essentially constant wall stress along the whole section of the slit. There is, however, a local stress concentration at the die exit and after this the stresses within the melt begin to relax as the polymer leaves the die. In the case of GAE (Fig. 5b), and for the same volumetric flow rate, the number of fringes observed downstream of the gas injection positions is greatly reduced and this corresponds to a matching reduction in wall stress.

The resulting extrudates were examined under SEM and the results at a high flow rate of 1.2 rpm and at 180 °C are shown in Fig. 6. The SEM images show no visible decrease in sharkskin with GAE. The reason for this can be explained as follows. Sharkskin defects are caused by the local stress concentrations that occur at the die exit. When gas is introduced, there is still a local stress concentration at the wall/ gas interface, but now this happens at the position of the gas injection. Therefore the local stress concentration still occurs with GAE and the sharkskin remains. This is confirmed both by experimental flow birefringence photographs in Fig. 5 and also by the Polyflow numerical simulations described below.

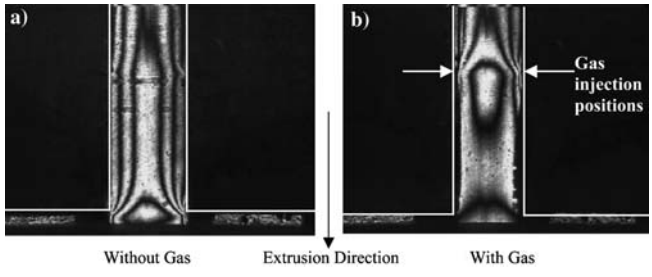

Fig. 5 Flow birefringence images for flow of Rigidex HDPE through Die I (die depth 15 mm, slit length 14.5 mm and gap width 3.9 mm) at 0.6 rpm and 180 °C **a** without gas and **b** with gas

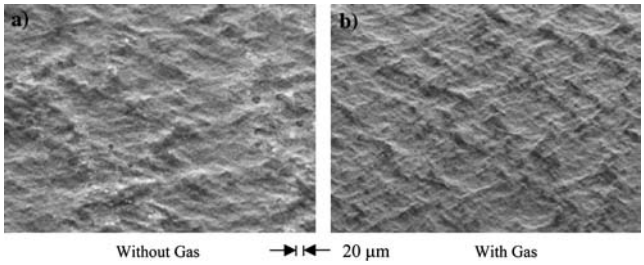

Fig. 6 SEM images of extrudate surfaces for Rigidex HDPE extruded though Die I at 1.2 rpm and 180 °C **a** without gas and **b** with gas

Figure 7 shows simulation results for the contours of PSD for the flow of Dowlex LLDPE through Die I, both with no slip and with full slip at the gas boundary layer. It can be seen that with no slip, a stress concentration is predicted at the die exit. With full slip, the stress concentration has been eliminated at the die exit but reappears at the point of gas injection. In order to examine PSDs closer to the wall, PSD values along a streamline 50 μm from the die wall were plotted as a function of position along the die. Figure 8a shows that with no slip, there are PSD peaks at the entry corner of the die and also a larger one at the die exit. Figure 8b shows that with full slip along the gas boundary, the PSD peak at the die entry corner is still present while the peak at the die exit disappears, but it has actually been moved to the point of gas injection. This explains why Die I did not eliminate sharkskin. The stress concentration causing the sharkskin was eliminated at the die exit but was moved upstream to the point of gas injection.

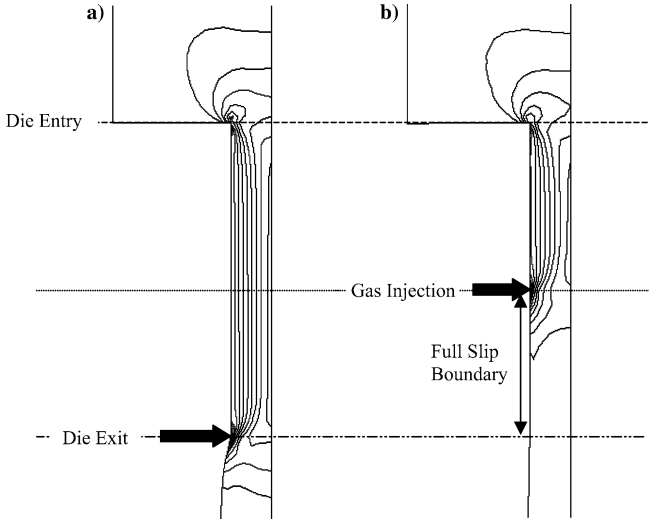

Fig. 7 Simulation results for contours of PSD in Dowlex LLDPE flowing through Die I at 2.4×10^{-7} m^3/s and 190 °C **a** with no slip at the wall and **b** with full slip along the gas boundary layer

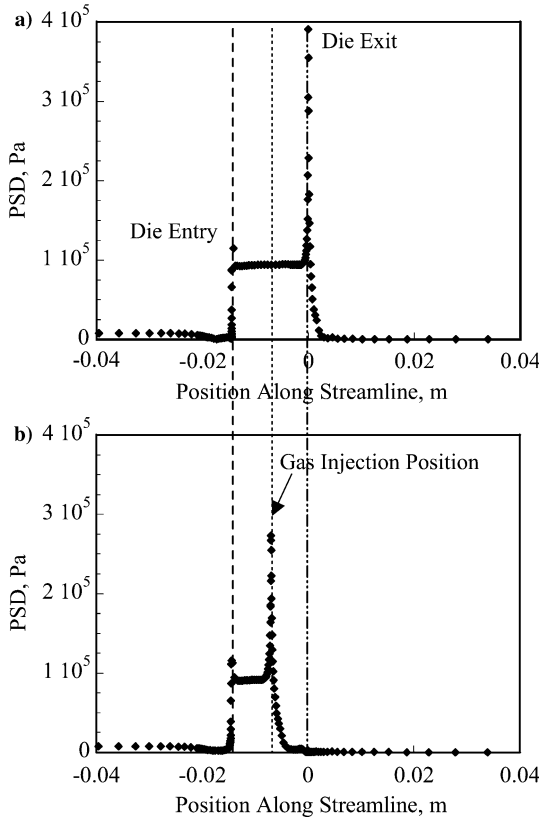

Fig. 8 Simulation results for PSD values along a streamline 50 μm from the die wall for Dowlex LLDPE flowing through Die I at 2.4×10^{-7} m^3/s and 190 °C **a** with no slip at the wall and **b** with full slip along the gas boundary layer

Die II

Simulations were then carried out to observe the effect of putting the gas injection points at an upstream position where the stress levels were low. This was compared with putting the injection point 4 mm from the die exit and also with no gas injection. Simulations were carried out assuming full slip at the gas boundaries. The meshes were designed with element sizes 30×30 μm at the die exit for the mesh designed for no slip and at the slip initiation point for the two other meshes. Figure 9 shows the stress field for these three cases and it can be seen that with no slip at the wall there is the usual stress concentration at the die exit; with full slip introduced at 4 mm from the exit, there is a stress concentration at the slip initiation point; when slip is introduced at an upstream position, the stress concentration at the slip initiation point is negligible and the highest stresses occur at the die contraction. Therefore positioning the gas injection points in the upstream die area should delay the onset of sharkskin to higher flow rates.

Figure 10 shows the PSD values along a streamline 50 μm from the die wall for the three cases. It can be seen from the figure that a high PSD peak occurs at

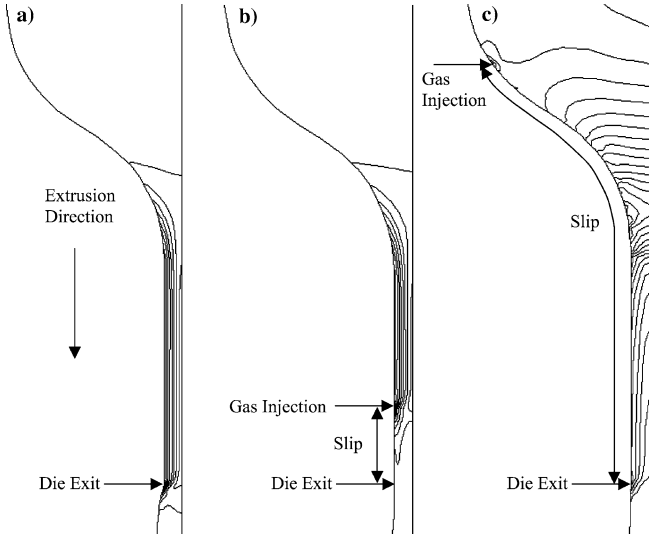

Fig. 9 Simulation results for contours of PSD in Dowlex LLDPE flowing through a curved entry 1.4 mm gap width die at 2.4×10^{-7} m^3/s and 190 °C **a** with no slip, **b** with slip 4 mm from the die exit and **c** with slip starting at an upstream position

the die exit for no wall slip; for full slip initiating 4 mm from the die exit, the PSD peak at the slip initiation point is still relatively high; however, for upstream slip, a peak stress does not occur at the slip initiation point, but the highest stresses occur further downstream at the die contraction and are much lower than for the preceding cases. This indicated that gas injection into the lower stress upstream region of the die would minimise the stress concentration.

A die was therefore designed with the gas injection positions slightly upstream of the die contraction (see Fig. 2). Experiments on this die were carried out using Rigidex HDPE at 180 °C and Dowlex LLDPE at 190 °C. The flow birefringence image in Fig. 11 shows the stress field in the Dowlex LLDPE melt without gas. The fringes indicate that at the positions of gas entry, the stresses are lower than after the die contraction. In terms of experimental realisation, it was discovered that the higher pressure at the upstream gas injection point resulted in unstable gas flow and it was not possible to establish a uniform and stable gas blanket at the wall. The gas tended to form bubbles in the melt and flowed through the melt in individual fingers down the die wall. Although a number of die designs were tested, stable upstream gas injection could not be achieved.

Partial slip simulations

In order to further investigate the effect of slip on stress concentrations, numerical simulations were carried out with varying levels of partial slip at a section of the die wall. The mesh used for this study is shown in Fig. 12. It

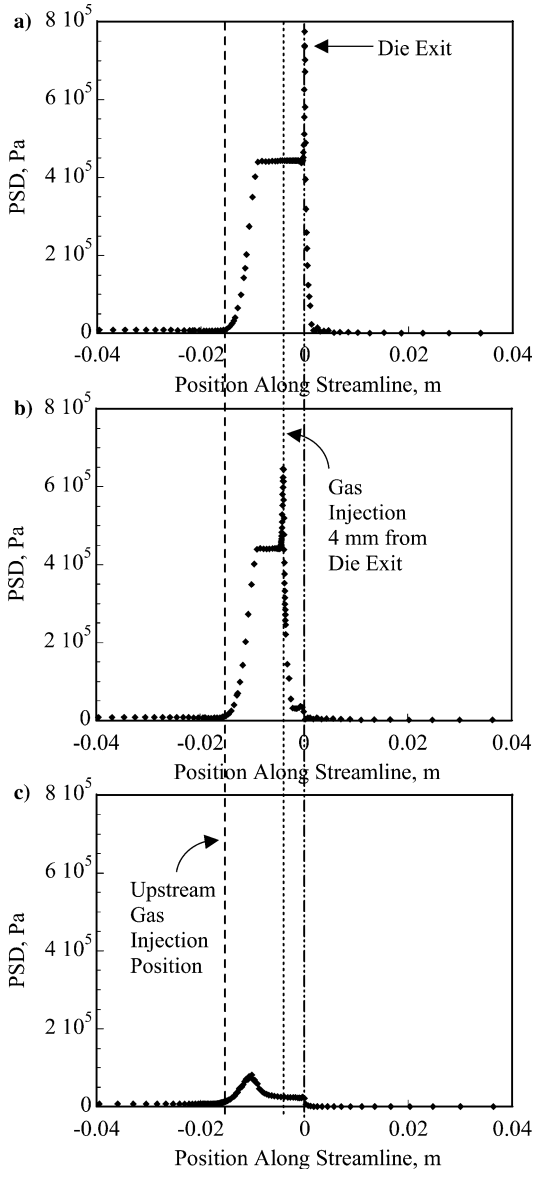

Fig. 10 Simulation results for PSD values along a streamline 50 μm from the die wall for Dowlex LLDPE flowing through a curved entry 1.4 mm gap width die at 2.4×10^{-7} m^3/s and 190 °C **a** with no slip at the wall, **b** with full slip 4 mm from die exit and **c** with upstream slip

was a parallel slit die with a 90 ° entry angle. The parameters used were for Dowlex at 190 °C. Simulations were carried out with varying slip coefficients. This gave rise to differing slip velocities and different PSD peaks at the slip initiation point and the die exit, as shown in Fig. 13.

The results from the simulations are summarised in Fig. 14, which shows a plot of PSD peaks at the die entry, exit and slip initiation point versus the ratio between the slip velocity and the centreline velocity. The plot shows that along the direction of increasing slip

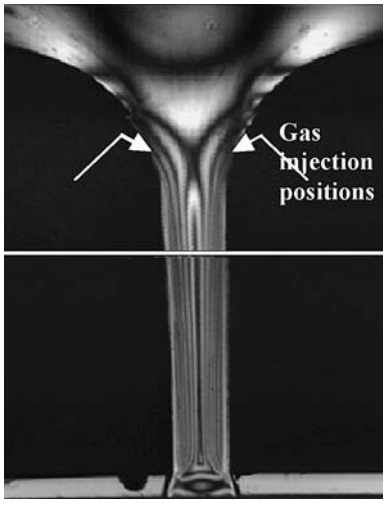

Fig. 11 Flow birefringence image of Dowlex LLDPE flowing through Die II at 0.6 rpm and 190 °C

(along the x-axis) the PSD peak at the die entry remains constant (as expected), the PSD peak at the slip initiation point increases and the PSD peak at the die exit decreases. Therefore, with partial slip, PSD peaks are smaller than for no slip or for full slip and a reduction in sharkskin would be expected. If the level of partial slip is too low, the PSD peak at the die exit is still high enough

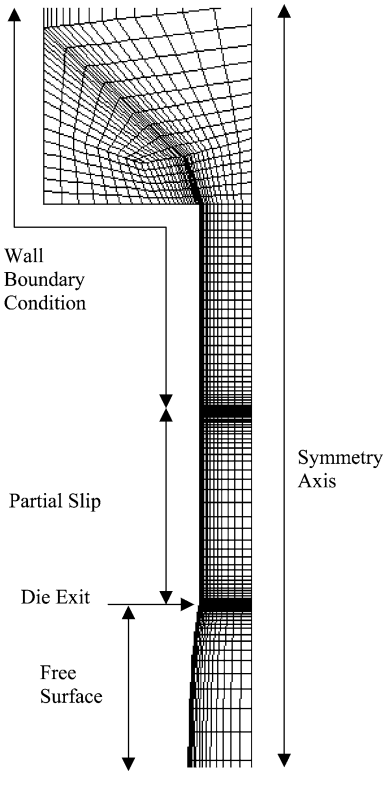

Fig. 12 Mesh used for numerical simulations of partial slip (2,180 elements)

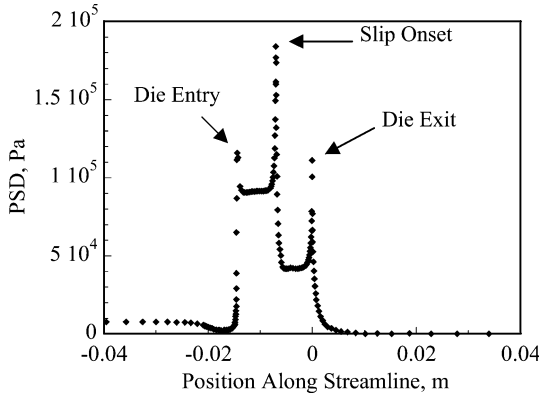

Fig. 13 PSD values for a partial slip of $f_{slip} = 8\times10^6$ along a streamline 50 μm from the die wall, simulated for Dowlex LLDPE at 190 °C

to cause sharkskin. If the level of partial slip is too high (as it was with GAE), the PSD peak at the slip initiation point becomes too high and again causes sharkskin. The plot also shows that a level of slip exists where PSD peaks at both the slip initiation point and the die exit are minimised (at $v_{slip}/v_{max} = 0.35$).

It has been recorded in the literature that increasing wall slip decreases sharkskin (see for example [16, 17]). Studies with PTFE and rubber coatings at the exit of the die have also shown that sharkskin can be eliminated with slip [18, 19]. A difference between PTFE or rubber coatings and GAE is that having GAE is equivalent to a full slip condition. The size of the stress concentration at the transition from stick to slip is therefore comparable to that at a die exit. GAE leads to a sharp stress concentration whereas for PTFE or rubber coatings, velocity profiles have shown that only a partial slip is imparted, and the transition from stick to slip is therefore not so sharp. Numerical simulations show that with partial slip the exit singularity is split into two smaller sub-singularities.

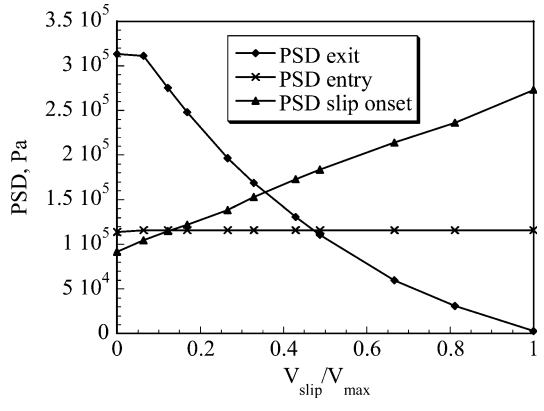

Fig. 14 A plot of PSD peaks at the die entry, die exit and at the slip initiation point versus increasing slip, simulated in Polyflow for Dowlex LLDPE at 190 °C at a flow rate of 2.4×10^{-7} m^3/s (typical experimental flow rate for extrusion of LLDPE within a sharkskin regime)

Furthermore, with GAE, once the sharkskin instability arises due to the slip initiation stress concentration, it is allowed to develop due to the free surface of the gas. However, with a PTFE or rubber surface the instability is not free to build up as it is constrained by the die. Polymer processing additives, on the other hand, are able to delay sharkskin more than PTFE coatings since they deposit and impart a partial slip along the whole of the die surface, as well as the extruder screw and barrel [16]. Therefore a stress concentration arises only at the die exit, and the magnitude of this stress concentration is lower than that for a die with no wall slip. The results presented in this paper have shown that having slip along the die wall will not necessarily reduce the sharkskin instability; for example, full slip as imparted by GAE does not reduce sharkskin. Factors of importance are the level of slip imparted and the condition of the subsequent wall boundary (whether it is solid or free).

Conclusions

Experimental and numerical simulation results reported in this paper show that gas injection in the parallel section of a slit die can move the stress concentration upstream to the gas injection point. In this case, sharkskin is therefore not reduced. This supports the view that local stress concentrations are responsible for the instability. Numerical simulations indicate that the stress concentrations can be significantly reduced if gas is injected at a low stress, upstream die entry region. It was, however, found experimentally that upstream gas injection could not be achieved in this study due to an inability to produce a stable gas flow. Numerical simulations of varying levels of partial slip along the die wall indicate that there is an optimum level of slip where the stress concentrations are minimised. This is believed to be a factor accounting for why coatings such as PTFE (which impart a partial slip) are able to eliminate sharkskin, whereas GAE (which imparts a full slip) is not.

Acknowledgements The authors would like to thank the EU for the funding of this project (Postpone Polymer Processing Instabilities (3PI) Competitive and Sustainable Growth), Cambridge Reactor Design (CRD) for help with the design and manufacture of gas injection dies, and Alan Heaver for help in obtaining SEM images.

References

1. Tordella JP (1969) Rheology, vol 5. Academic, New York
2. Petrie CJS, Denn MM (1976) Instabilities in polymer processing. AIChE J 22(2):209–236
3. Larson RG (1992) Instabilities in viscoelastic flow. Rheol Acta 31:213–263
4. Wang SQ (1999) Molecular transitions at polymer/wall interfaces: origins of flow instabilities and wall slip. Adv Polym Sci 138:227–275
5. Denn MM (1990) Issues in viscoelastic fluid mechanics. Annu Rev Fluid Mech 22:13–34
6. Denn MM (1992) Surface-induced effects in polymer melt flow. In: Moldenaers P, Keunings R (eds) Theoretical and applied rheology. Proc XIth Int Congress on Rheology. Elsevier, New York, pp 45–49
7. Denn MM (2001) Extrusion instabilities and wall slip. Annu Rev Fluid Mech 33:265–297
8. Rutgers RPG, Mackley MR (2000) The correlation of experimental surface extrusion instabilities with numerically predicted exit surface stress concentrations and melt strength for linear low-density polyethylene. J Rheol 44(6):1319–1334
9. Piau JM, El Kissi N, Toussaint F, Mezghani A (1995) Distortions of polymer melt extrudates and their elimination using slippery surfaces. Rheol Acta 34:40–57
10. Migler KB, Lavallee C, Dillon MP, Woods SS, Gettinger CL (2001) Visualizing the elimination of sharkskin through fluoropolymer additives: coating and polymer–polymer slippage. J Rheol 45(2):565–581
11. Liang RF, Mackley MR (2001) The gas-assisted extrusion of molten polyethylene. J Rheol 45:211–226
12. Arda DR (2003) The sharkskin extrusion instability and its minimisation in polyethylene processing. PhD Thesis, University of Cambridge, Cambridge, UK
13. Crochet MJ, Walters K (1993) Computational rheology—a new science. Endeavour 17(2):64–77
14. Lipscomb GG, Keunings R, Denn MM (1987) Implications of boundary singularities in complex geometries. J Non Newton Fluid Mech 24(1):85–96
15. Renardy M (2000) Current issues in non-Newtonian flows: a mathematical perspective. J Non Newton Fluid Mech 90(2–3):243–259
16. Stewart CW (1993) Wall slip in the extrusion of linear polyolefins. J Rheol 37(3):499–513
17. Venet C, Vergnes B (1997) Experimental characterization of sharkskin in polyethylenes. J Rheol 41(4):873–892
18. Barone JR, Plucktaveesak N, Wang SQ (1998) Interfacial molecular instability mechanism for sharkskin phenomenon in capillary extrusion of linear polyethylenes. J Rheol 42(4):813–832
19. Kulikov O, Hornung K (2003) A simple way to suppress surface defects in the processing of polyethylene. In: Proc 12th Int Conf on Deformation, Yield and Fracture of Polymers, 7–10 April 2003, Cambridge, UK, pp 411–414